Published OnlineFirst June 12, 2019; DOI: 10.1158/2326-6066.CIR-18-0896

Research Article

Cancer Immunology Research

High Numbers of Circulating CD57$^+$ NK Cells Associate with Resistance to HER2-Specific Therapeutic Antibodies in HER2$^+$ Primary Breast Cancer

Aura Muntasell[1], Sònia Servitja[2,3], Mariona Cabo[1], Begoña Bermejo[4], Sandra Pérez-Buira[5], Federico Rojo[5], Marcel Costa-García[6], Oriol Arpí[2], Manuela Moraru[7], Laia Serrano[8], Ignasi Tusquets[2,3,6], María Teresa Martínez[4], Gemma Heredia[6], Andrea Vera[1], María Martínez-García[2,3], Laura Soria[1], Laura Comerma[8], Sara Santana-Hernández[1], Pilar Eroles[4,9], Ana Rovira[2,3], Carlos Vilches[7], Ana Lluch[4,9,10], Joan Albanell[2,3,6], and Miguel López-Botet[1,6]

Abstract

Natural killer (NK) cells can orchestrate effective antitumor immunity. The presence of tumor-infiltrating NK cells in diagnostic biopsies predicts pathologic complete response (pCR) to HER2-specific therapeutic antibodies in patients with primary breast cancer. Here, we analyzed whether diversity in circulating NK cells might influence tumor infiltration and HER2-specific therapeutic antibody efficacy. We found that numbers of circulating CD57$^+$ NK cells inversely correlated with pCR to HER2-specific antibody treatment in patients with primary breast cancer independently of age, traditional clinicopathologic factors, and CD16A 158F/V genotype. This association was uncoupled from the expression of other NK-cell receptors, the presence of adaptive NK cells, or changes in major T-cell subsets, reminiscent of cytomegalovirus-induced immunomodulation. NK-cell activation against trastuzumab-coated HER2$^+$ breast cancer cells was comparable in patients with high and low proportions of CD57$^+$ NK cells. However, circulating CD57$^+$ NK cells displayed decreased CXCR3 expression and CD16A-induced IL2-dependent proliferation *in vitro*. Presence of CD57$^+$ NK cells was reduced in breast tumor–associated infiltrates as compared with paired peripheral blood samples, suggesting deficient homing, proliferation, and/or survival of NK cells in the tumor niche. Indeed, numbers of circulating CD57$^+$ were inversely related to tumor-infiltrating NK-cell numbers. Our data reveal that NK-cell differentiation influences their antitumor potential and that CD57$^+$ NK cells may be a biomarker useful for tailoring HER2 antibody–based therapeutic strategies in breast cancer.

[1]Immunity and Infection, IMIM (Institut Hospital del Mar d'Investigacions Mèdiques), Barcelona, Spain. [2]Cancer Research Program, IMIM (Institut Hospital del Mar d'Investigacions Mèdiques), Barcelona, Spain. [3]Department of Medical Oncology, Hospital del Mar-CIBERONC, Barcelona, Spain. [4]Department of Oncology, Hospital Clinico de Valencia-CIBERONC, Valencia, Spain. [5]Department of Pathology, IIS "Fundacion Jimenez Diaz University Hospital," Madrid, Spain. [6]Universitat Pompeu Fabra, Barcelona, Spain. [7]HLA-Immunogenetics Department, Instituto Hospital Universitario Puerta de Hierro, Majadahonda, Spain. [8]Department of Pathology, Hospital del Mar, Barcelona, Spain. [9]Biomedical Research Institute, INCLIVA, Valencia, Spain. [10]Universitat de Valencia, Valencia, Spain.

Note: Supplementary data for this article are available at Cancer Immunology Research Online (http://cancerimmunolres.aacrjournals.org/).

A. Muntasell and S. Servitja contributed equally to this article.

J. Albanell and M. López-Botet are the co-senior authors of this article.

Corresponding Authors: Aura Muntasell, IMIM (Hospital del Mar Medical Research Institute), Barcelona 08003, Spain. Phone: 349-3316-0811; Fax: 349-3316-0901; E-mail: amuntasell@imim.es; and Joan Albanell, jalbanell@hospitaldelmar.cat

Cancer Immunol Res 2019;7:1280–92

doi: 10.1158/2326-6066.CIR-18-0896

Introduction

Natural killer (NK) cells are innate lymphocytes that can recognize antibody-coated tumor cells via the activating Fcγ receptor CD16A (FcγRIIIA), leading to tumor cell death by antibody-dependent cellular cytotoxicity (ADCC) and the release of immune cell recruiting chemokines and proinflammatory cytokines (1–5). In experimental breast cancer models, NK cells command antitumor adaptive immunity and contribute to the antitumor activity of HER2-specific antibodies (6–9). In patients, indirect evidence suggests that NK cells influence the efficacy of anti-HER2 therapeutic antibodies such as trastuzumab and pertuzumab, which are the standard of care in HER2$^+$ breast cancer. An increase in tumor-infiltrating NK cells was reported after trastuzumab-docetaxel and T-DM1 (a trastuzumab–emtansine conjugate) treatment (10, 11). We have described an association between tumor-infiltrating NK-cell numbers in diagnostic biopsies and the achievement of pathologic complete responses (pCR) to HER2-specific antibody-based treatment in patients with HER2$^+$ breast cancer (12). Despite this evidence supporting a role for NK-cell–mediated ADCC in the efficacy of anti-HER2 therapeutic antibodies, little is known about whether

Published OnlineFirst June 12, 2019; DOI: 10.1158/2326-6066.CIR-18-0896

human NK-cell diversity influences NK-cell homing to and function in solid tumors.

In healthy adults, approximately 90% of NK cells in peripheral blood belong to the cytotoxic CD56^{dim}CD16$^+$ subpopulation capable of developing ADCC responses, whereas approximately 10% constitute the CD56^{bright}CD16$^{-/low}$ subset characterized by their cytokine production and preferential homing to secondary lymphoid organs (13). CD56^{dim}CD16$^+$ NK cells include several subsets identified by distinct receptor combinations and differentiation status. Genetic (i.e., KIR and HLA haplotypes) and environmental factors, including infection by human cytomegalovirus (HCMV), respectively, shape the steady-state distribution of the NK-cell receptor repertoire and the development of circulating NK-cell subsets with adaptive features (14–17). HCMV-induced adaptive NK cells, identified by elevated expression of the activating receptor CD94/NKG2C, among other phenotypic and epigenetic features, display enhanced ADCC responses in several *in vitro* experimental models (18–20). Biological age is another factor associated with changes in the composition of the human NK-cell repertoire (21, 22). The CD57 epitope is a glycan carbohydrate (23) labeling differentiated NK cells, with variable prevalence in the adult CD56^{dim} CD16$^+$ NK-cell repertoire (24, 25). CD57 expression is low in newborn NK cells, increases with age (26–28), and has been associated with chronic viral infections (29). CD57$^+$ NK cells display lytic activity when stimulated through CD16 yet reduced proliferative capacity in response to cytokines (24, 30). A polymorphism in the gene encoding CD16A (*FCGR3A)*, which results in two receptor variants with different affinities for IgG1, also modulates NK-cell–mediated ADCC responses (31).

We hypothesized that the configuration of the circulating NK-cell repertoire could influence the composition of tumor-infiltrating NK cells and hence, the efficacy of HER2-specific antibody-based treatment in breast cancer. We approached this question by an integrated analysis of: (i) the relationship between the phenotype of circulating NK cells, the CD16A 158V/F genotype, and efficacy outcomes in a prospective cohort of patients with HER2$^+$ breast cancer with primary disease receiving neoadjuvant treatment with HER2-specific antibodies; (ii) the comparison of circulating and tumor-associated NK cells by IHC on FFPE tumor biopsies as well as by multiparametric flow cytometry in fresh *ex vivo* samples; and (iii) the evaluation of NK-cell function, proliferation, and survival in *in vitro* assays.

Table 1. Patient characteristics

	Cohort
No. of patients	66
Mean age	58
Tumor size (*n*/%)	
T1–T2	51 (77%)
T3–T4	15 (23%)
Lymph node status (*n*/%)	
N0	25 (38%)
N+	41 (61%)
Histologic type (*n*/%)	
DIC	58 (87%)
Others	8 (10%)
Histologic grading (*n*/%)	
G1–G2	33 (50%)
G3	30 (45%)
NA	3 (4%)
Hormonal status (*n*/%)	
ER$^+$	47 (71%)
ER$^-$	19 (29%)
PR$^+$	30 (45%)
PR$^-$	36 (55%)
Ki67 Index (*n*/%)	
<20%	8 (12%)
≥20%	57 (86%)
NA	1 (1%)
Anti-HER2 (*n*/%)	
Trastuzumab	45 (69%)
Dual anti-HER2	20 (31%)
Chemo regimen (*n*/%)	
Anthracylines and taxanes	43 (73%)
Taxanes	12 (20%)
Hormonal	4 (7%)
pCR	
pCR	27 (41%)
No pCR	37 (56%)
NA	2 (3%)
Clinical follow-up	
Median (IQR)	26 (20–33)

NOTE: Dual anti-HER2 includes: trastuzumab + pertuzumab ($n = 17$), trastuzumab + lapatinib ($n = 2$), and trastuzumab + neratinib ($n = 1$).

Methods

Study design

The conformation of the NK-cell receptor repertoire was analyzed in baseline peripheral blood samples from patients prospectively recruited between October 2013 and December 2016 at Hospital del Mar (Barcelona, Spain) and Hospital Clínic de Valencia (Valencia, Spain; prospective cohort $n = 66$). Cohort diagram and characteristics are summarized in Supplementary Fig. S1 and Table 1. Patients included newly diagnosed, previously untreated, primary breast cancer cases. HER2$^+$ subtype classification was defined following 2013 American Society of Clinical Oncology/College of American Pathologists guidelines (32). All patients received a neoadjuvant combination therapy of standard chemotherapy and HER2-specific antibodies. Pathologic response at surgery after completing the neoadjuvant treatment was reported according to Miller–Payne grading system. Grades 1–4 are categorized as a partial pathologic response and grade 5 as pCR. The primary efficacy endpoint in our study was pCR defined as ypT0ypN0 [i.e., no malignant invasive cells identifiable in sections from the site of the tumor (T0) and axillary lymph nodes (N0); only vascular fibroelastotic stroma] based on histopathologic analysis of the resection specimen (33); disease-free survival (DFS) was calculated as the time from surgery until any breast cancer relapse or death by any cause. An extended T-cell immunophenotype was analyzed in a subset of 22 patients selected on the basis of their proportions of circulating CD57$^+$ NK cells according to cut-off values providing the best Youden index for pCR: <65% CD57$^+$ NK cells corresponding to CD57^{low} and ≥65% CD57$^+$ NK cells to CD57^{high}.

The study was conducted following Declaration of Helsinki guidelines. All patients and healthy volunteers gave informed consent for the analysis of peripheral blood and tumor biopsies for research purposes and biomarker assessment. This study was approved by the Hospital del Mar Ethics Committee (2013/5307) and is reported according to the REMARK guidelines.

Immunophenotypic analysis by flow cytometry

Blood samples obtained by venous puncture in EDTA tubes at diagnosis were fractionated to obtain a basic hemogram

Published OnlineFirst June 12, 2019; DOI: 10.1158/2326-6066.CIR-18-0896

and viable peripheral blood mononuclear cells (PBMC), which were cryopreserved for later use. Phenotypic analyses of baseline PBMC samples were performed following standard flow cytometry protocols. Briefly, PBMCs were pretreated with aggregated human IgG, incubated with individual unlabeled specific mAbs, washed and further incubated with the secondary PE-Cy7–conjugated F(ab')2 polyclonal goat anti-mouse IgG or IgM. Subsequently, samples were stained with combinations of directly labeled antibodies. Prior to intracellular staining with anti-FcRγ-FITC, samples were fixed and permeabilized (fixation/permeabilization kit, BD Biosciences).

Antibodies used include anti-CD45-AlexaFluor700 (clone 2D1), anti-CD56-APC (clone CMSSB), anti-CD16-APC-Cy7 (clone CB16), anti-CX3CR1-PE-Cy7 (clone 2A9-1) and anti-CXCR3-efluor660 (clone CEW33D) from eBiosciences; anti-CXCR1-PE (clone 8F1) from BioLegend; anti-CD3-PerCP (clone SK7), anti-CD45RA-FITC (clone L48), anti-CD4-allophycocyanin (APC; clone SK3), anti-CCR7-PE-Cy7 (clone 3D12), anti-CD8-HV500 (clone RPA-T8), anti-CD28-PE-CF594 (clone CD28.2) from BD Biosciences; anti-NKG2C- Phycoerythrin (PE; clone 134591) from R&D Systems, and anti-FcεR γ subunit-FITC (polyclonal) from Merck Millipore. Anti-LILRB1 (clone HP-F1), anti-NKG2A (clone Z199) provided by Dr. A. Moretta, University of Genoa, Genoa, Italy; anti-CD57 (clone HNK1) and anti-KIR3DL1 (clone DX9) provided by Dr. L. Lanier, University of California, San Francisco (San Francisco, CA); anti-KIR2DL2/S2/L3 (clone CH-L) provided by Dr. S. Ferrini, National Institute for Cancer Research, Genoa, Italy; and anti-KIR2DL1 (clone DM-1) were produced in our laboratory and used either as cell culture supernatants or upon conjugation to fluorescein (FITC) or Pacific Blue (PB).

Data were acquired on an LSR Fortessa flow cytometer (BD Biosciences) and analyzed with FlowJo software (v10.0.7, Tree Star). All immunophenotypes were performed and analyzed blinded to the study endpoint. Expression of distinct markers was referred to $CD56^{dim}$ NK cells. Circulating NK-cell absolute numbers were calculated on the basis of hemogram counts and expressed as cells/μL of blood.

Trastuzumab-induced NK-cell ADCC *in vitro* assays with patient-derived PBMCs

For some patients, measurements of NK-cell degranulation (anti-CD107a-FITC, BD Biosciences) and intracellular TNFα (infliximab-Pacific Blue) were analyzed in baseline PBMC samples after 4-hour coculture with trastuzumab-coated SKBR3 cells (a human breast cancer cell line that overexpresses HER2) using standard flow cytometry protocols.

CD16A 158 V/F genotyping

DNA was isolated from total blood using the Pure gene Blood-Core kit B (Qiagen). Functional polymorphisms of FCGR3A, CD16A 158 V/F were determined using a PCR with confronting two-pair primers, as described previously (34). Because of the limited cohort size, influence of CD16A 158 V/F genotype has been analyzed by comparing those patients harboring the high-affinity allele (CD16 158V/V and V/F genotypes) to those homozygous for the low-affinity allele (CD16 158 F/F genotype).

Tumor-associated NK-cell phenotype

Presence of $CD57^+$ NK cells was evaluated in tumor-associated and circulating NK-cell paired samples from treatment-naïve breast cancer patients with primary disease undergoing surgical resection at Hospital del Mar (Barcelona, Spain; $n = 6$). For tumor-associated NK-cell characterization, a section within the core of the malignant area was selected by the pathologist and cleared of fat tissue prior to mechanical disruption. Tumor was digested for 40 minutes under agitation with collagenase type IV (1 mg/mL; Gibco) and DNAse (25U/mL; Sigma Aldrich). After filtration, single cell suspensions were stained with specific antibodies and analysed by multiparametric flow cytometry. vi-Stochastic neighbor embedding (SNE) methodology was implemented for the analysis of $CD57^+$ distribution in paired samples of tumor-associated and circulating lymphocytes (35). Raw flow cytometry data were imported into R using flowCore and openCyto packages. A compensation matrix generated in FlowJo (v10.0.7, Tree Star) was exported an applied into R. Lymphocytes were gated by forward and side scatter in the $CD45^+$ alive gate. Data from 10,000 gated lymphocytes or 2,000–5,000 NK cells were concatenated. Barnes-Hut t-SNE was conducted using the Rtsne package. Graphics were produced using packages ggplot2 and RColorBrewer.

NK-cell proliferation assays

For proliferation assays, NK cells were purified from CFSE-labeled PBMC [CFDA SE Cell trace (CFSE), Invitrogen, Molecular Probes] by negative selection using a Human NK Cell Enrichment kit (Miltenyi Biotec) and cultured in complete RPMI medium supplemented with 200 U/mL rhIL2 (Proleukin, Chiron) in flat-bottom 96-well plates previously coated with anti-CD16 (clone KD1). After 6 days, cells were surface stained with anti-CD56-APC and anti-CD57-BV605 (clone NK-1, BD Biosciences) and analyzed by flow cytometry. Results were expressed as percent of NK cells undergoing $\geq$4 divisions.

Tumor-infiltrating NK-cell numbers in diagnostic biopsies

Data on tumor stromal-infiltrating NK-cell (TI-NK) numbers as determined by the enumeration of $CD56^+CD3^-$ cells by IHC in diagnostic tumor biopsies was available from a previous study including a partially overlapping cohort of patients with $HER2^+$ primary breast cancer (12). The concordance between 40 of the patients included in both studies enabled the analysis of the relationship between $CD57^+$ NK-cell numbers and tumor-infiltrating NK cells presented here.

Statistical analysis

Bivariate analyses by Mann–Whitney *U* test were used to assess the putative association between pCR and NK-cell markers as continuous variables. Multivariate analysis was conducted with binary logistic regression by adding patient age (as continuous variable) and estrogen receptor status (ER^+ vs. ER^-) in the model, separately. Thresholds for $CD57^+$ NK-cell frequencies and numbers that best discriminated pCR achievement were determined using receiver operating characteristic (ROC) curve analysis and optimal cutoffs defined by the maximum Youden index. Predictive effects on pCR of $CD57^+$ NK cells as categorical variables were calculated by Fisher exact test. Cox proportional hazards regression was used to estimate the HR in DFS analysis. Kaplan–Meier curves for DFS were used to compare time to event in patients stratified by their pCR achievement or $CD57^+$ circulating NK cells. All *P* values were two-sided; *P* values lower than 0.05 were considered significant. Statistical analysis was performed using

Published OnlineFirst June 12, 2019; DOI: 10.1158/2326-6066.CIR-18-0896

GraphPad Prism version 6 (GraphPad software) and STATA version 15 (STATA Corp.).

Results

Circulating CD57$^+$ NK cell numbers associate with resistance to HER2-specific antibody treatment

The phenotype of circulating NK cells was studied by multiparametric flow cytometry in baseline PBMC samples from prospectively recruited patients with HER2$^+$ breast cancer, undergoing neoadjuvant treatment with HER2-specific antibodies and chemotherapy ($n = 66$). The analysis included several NK-cell receptors defining distinct NK-cell subsets (NKG2A, KIR2D, KIR3DL1, CD16, and NKG2C) and additional molecules associated with NK-cell differentiation (LILRB1, FcεRγ, and CD57; gating strategy in Supplementary Fig. S2). Clinicopathologic characteristics of the patient cohort are presented in Table 1. pCR to neoadjuvant treatment was confirmed in 42% (27/64) of patients; ER status was the only conventional factor significantly associated with pCR in the studied cohort [OR 6.89; 95% confidence interval (CI), 2.06–23.05; $P = 0.002$]. No significant differences were observed in total lymphocyte counts, total NK cells, or in the distribution of most NK-cell receptors (e.g., NKG2A and KIR2D) between patients achieving pCR or not, in response to HER2-specific antibody treatment (Fig. 1A; Supplementary Table S1). Higher LILRB1$^+$ and lower CD57$^+$ average proportions of NK cells were detected in patients achieving pCR. However, absolute CD57$^+$ NK-cell counts were the only parameter significantly different between patients achieving pCR or not. Despite the positive correlation between CD57$^+$ NK cells and age ($r = 0.44$ and $r = 0.46$, for relative and absolute numbers, respectively, $P = 0.002$), CD57$^+$ NK-cell numbers independently associated with lower likelihood of response to HER2-specific antibodies when adjusting by age [%CD57$^+$ NK cells OR 1.04 (95% CI, 1.007–1.09), $P = 0.01$; CD57$^+$ NK cells/μL OR 1.006 (95% CI, 1.0004–1.01), $P = 0.03$] and ER status [%CD57$^+$ NK cells OR 1.05 (95% CI, 1.01–1.09), $P = 0.01$; CD57$^+$ NK cells/μL OR 1.007 (95% CI, 1.0008–1.01), $P = 0.02$, per unit increase] in multivariate analysis. Higher frequencies of CD57$^+$ NK cells were detected in patients with G1–G3 responses according to Miller–Payne criteria (Fig. 1B), hence identifying patients resistant to HER2-specific antibody–based neoadjuvant treatment. CD57$^+$ NK-cell numbers were not associated with any clinicopathologic factor [i.e., tumor size, tumor grade, hormone receptor status (Supplementary Fig. S3A–S3D)]. ROC curves and cut-off values providing best discrimination between pCR and non pCR for CD57$^+$ circulating NK cells were calculated (Supplementary Fig. S3E). As categorical variables, pCR rates were 60% in patients with <65% as compared with 10% in patients with ≥65% circulating CD57$^+$ NK cells (Fig. 1C). Concordantly, pCR rates in patients with <164 CD57$^+$ NK cells/μL were 60%, whereas only 18% of patients with ≥164 circulating CD57$^+$ NK cells/μL achieved pCR (Fig. 1C).

Frequencies of circulating CD57$^+$ NK cells in baseline samples from patients with HER2$^+$ breast cancer were comparable with those detected in a sample of age-matched controls ($n = 15$), previously characterized in our laboratory (Supplementary Fig. S4).

None of the markers analyzed in NK cells and T cells correlated with disease-free survival (DFS) in linear regression analysis (Supplementary Table S1B and S2). Nonetheless, because pCR in the primary tumor is associated with long-term outcome in HER2$^+$ breast cancer (36), we analyzed the association between CD57$^+$ NK cells as categorical variable and DFS. In Kaplan–Meier analysis, patients with low CD57$^+$ NK cells (<65% and <164 cells/μL; Fig. 1D–F) showed a trend for prolonged DFS yet not reaching statistical significance perhaps due to the small number of events guiding these analyses (5 relapses of 64 patients).

The association between CD57$^+$ NK cells and response to anti-HER2 is unrelated to HCMV-induced immunomodulation

Chronic infection by HCMV has been associated with the persistent expansion of NKG2C$^+$ adaptive NK-cell subpopulations including high proportions of CD57$^+$ and FcRγ-deficient cells (30, 37, 38) and the inflation of CD57$^+$ effector memory T cells with a terminal differentiation phenotype (39). We next assessed whether elevated CD57$^+$ NK-cell numbers in the studied patient cohort could be related to HCMV-induced immunomodulation. HCMV seroprevalence was 86% in the analyzed cohort. As shown in Supplementary Fig. S5A and S5B, frequencies of NKG2C$^+$ and FcRγ$^-$ adaptive NK cells were comparable in patients achieving or not pCR to HER2-specific antibody–based treatment. Indeed, patients with high frequencies of CD57$^+$ NK cells showed variable proportions of NKG2C$^+$ NK cells, despite the positive correlation between both NK-cell markers (Supplementary Fig. S5C, gray area). On the other hand, proportions of CD57$^+$ NK cells and HCMV-specific IgG titers did not correlate (Supplementary Fig. S5D) and CD57$^+$ T-cell numbers were not associated with pCR achievement in these patients (Supplementary Table S2). An analysis of the T-cell compartment was done in a fraction of patients selected on the basis of their CD57$^+$ NK-cell phenotypes ($n = 22$). The distribution of naïve, central memory (CM), effector memory (EM), and terminally differentiated effector memory (EMRA) CD8$^+$ T cells, as identified by CD45RA and CCR7 expression, was comparable in patients with low (<65%) or high (≥65%) proportions of CD57$^+$ NK cells (Supplementary Fig. S5E and S5F). Similarly, total CD8$^+$ and CD4$^+$ T cells as well as frequencies of CD57$^+$ and CD28$^-$ terminally differentiated CD8$^+$ T lymphocytes were comparable between both patient groups (Supplementary Fig. S5E–S5G).

These analyses indicate that the association between CD57$^+$ NK cells and the efficacy of HER2-specific antibodies in patients with breast cancer appears uncoupled from the expansion of adaptive NK cells and gross changes in the distribution of CD8$^+$ T-cell subsets, reported to be associated with HCMV-dependent immunomodulation.

The association of CD57$^+$ NK cells with response to anti-HER2 is independent of CD16A 158V/F genotypes

Improved responses to HER2-specific antibody-based treatments have been described for patients with CD16A 158V/F and 158V/V genotypes in some studies but not in others (40–42). Considering that circulating CD57$^+$ NK cells express the CD16 receptor, we analyzed whether the CD16A 158V/F genotype could influence the association between baseline CD57$^+$ NK cells and response to treatment with HER2 therapeutic antibodies. In our patient cohort, CD16A 158 V/V, CD16A 158 V/F, and CD16A 158 F/F genotypes, respectively, represented 15% ($n = 9$), 34% ($n = 20$), and 51% ($n = 30$) of the studied population, in conformance with the Hardy–Weinberg equilibrium (MAF: 0.32).

Published OnlineFirst June 12, 2019; DOI: 10.1158/2326-6066.CIR-18-0896

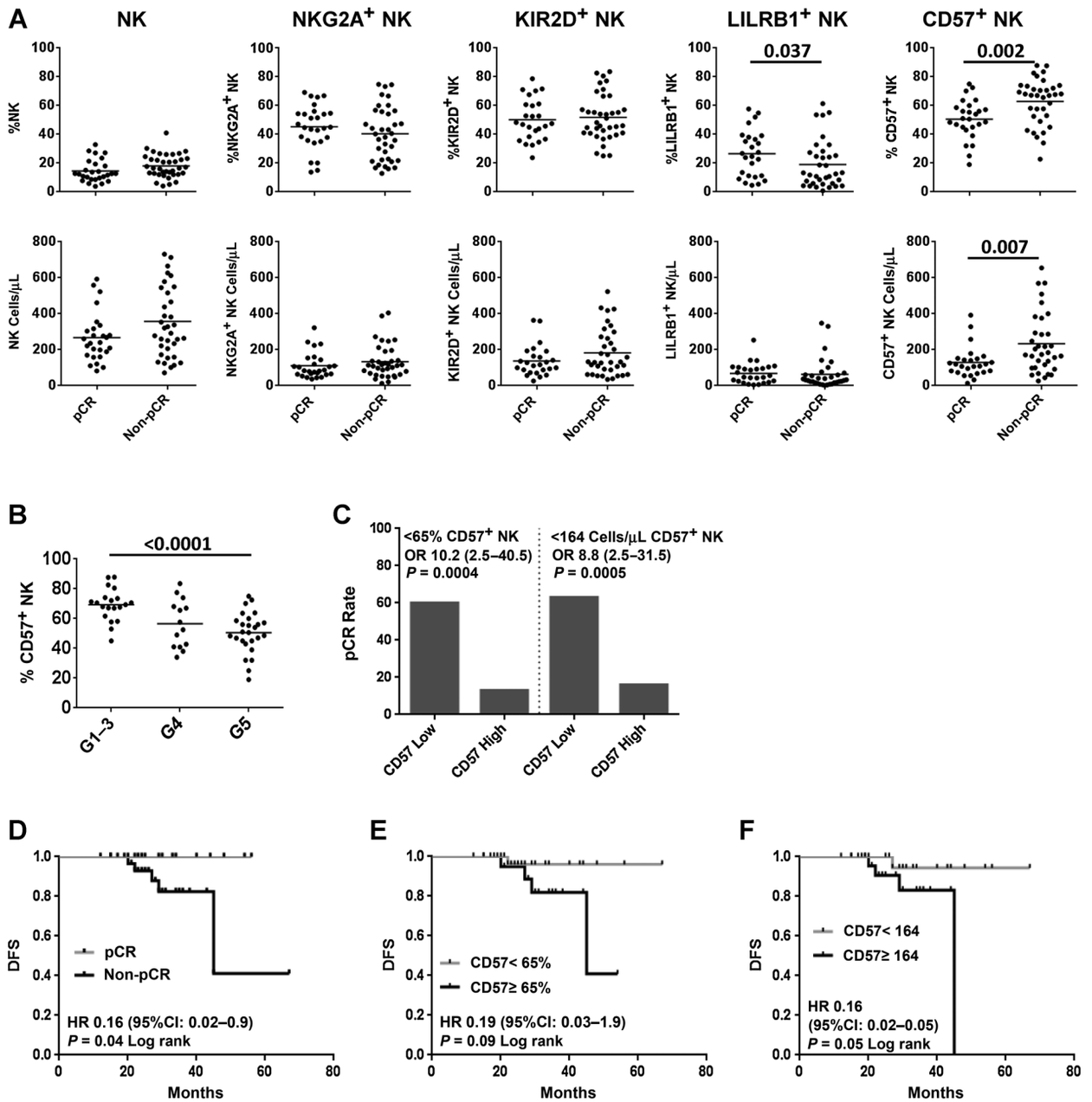

Figure 1.

Baseline CD57$^+$ NK cells associate with pCR in patients with HER2$^+$ breast cancer treated with neoadjuvant HER2-specific antibody–based treatment. The NK-cell phenotype was analyzed by multiparametric flow cytometry in baseline PBMC samples from patients with HER2$^+$ breast cancer. **A,** Frequencies and absolute numbers of total, CD57$^+$, NKG2A$^+$, and KIR2D$^+$ (including KIR2DL1$^+$ and KIR2DL2/L3/S2$^+$ NK cells as identified by the combination of DM-1 and CHL mAbs) and LILRB1$^+$ NK cells in patients stratified by pCR to treatment including HER2-specific antibodies. **B,** Proportions of CD57$^+$ NK cells in patients categorized by their response to treatment according to Miller–Payne criteria. **C,** pCR rates in patients stratified according to CD57$^+$ NK-cell cutoffs. Patients with $<$ or $\geq$ 65% and 164 cells/µL are labeled as CD57^{low} and CD57^{high}, respectively. ORs and 95% CIs for pCR are indicated. Kaplan–Meier curves for DFS in patients stratified for pCR to neoadjuvant treatment (**D**) as well as by baseline proportions of CD57$^+$ NK cells ($\geq$ and $<$ 65%; **E**), or CD57$^+$ NK-cell numbers ($\geq$ and $<$ 164 NK cells/µL; **F**).

Clinicopathologic characteristics of patients with CD16 158 V/V and V/F versus CD16 158 F/F genotypes were comparable (Supplementary Table S3). A trend for higher pCR rate in CD16A 158 V/V and V/F as compared with F/F patients was not statistically significant [2.2 OR (95% CI, 0.777–6.23), $P = 0.13$; Fig. 2A]. *In vitro* degranulation assays confronting patient-derived PBMCs with trastuzumab-coated SKBR3 cells showed that NK-cell–mediated ADCC was lower in patients with CD16A 158 F/F as compared to patients with CD16A 158 V/V or V/F genotypes (Fig. 2B). However, average frequencies and numbers of CD57$^+$ NK cells were comparable in patients encoding CD16A 158 V/V or V/F and CD16A 158F/F genotype (Fig. 2C and D). The association

Published OnlineFirst June 12, 2019; DOI: 10.1158/2326-6066.CIR-18-0896

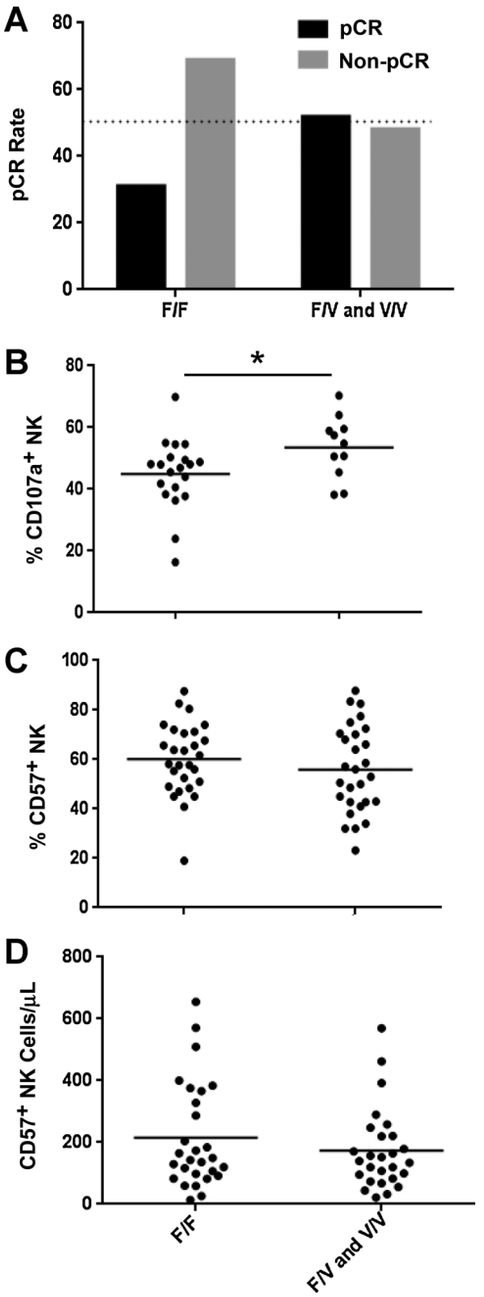

Figure 2.

pCR achievement, trastuzumab-induced NK-cell activation, and CD57$^+$ NK cells in breast cancer patients with distinct CD16A 158V/F genotype. The CD16A 158V/F genotype was analyzed in DNA samples from patients with primary HER2$^+$ breast cancer ($n = 60$) by PCR. **A,** pCR rates in patients categorized according to their CD16A 158F/F or CD16A 158V/V and V/F genotypes. **B,** NK-cell degranulation analyzed in baseline PBMC samples from patients with HER2$^+$ breast cancer upon coculture with trastuzumab-coated SKBR3 cells by flow cytometry. Percentage of CD107a$^+$ CD56^{dim} NK cells in response to trastuzumab-coated SKBR3 cells in patients with CD16 158 F/F ($n = 20$) as compared with patients harboring CD16 158 V/F or V/V genotype ($n = 21$). *P* values calculated by Mann–Whitney *U* test. **C** and **D,** Relative and absolute numbers of circulating CD57$^+$ NK cells in baseline samples from patients stratified by their CD16 158V/F genotype ($^*P < 0.05$; Mann–Whitney test).

between circulating CD57$^+$ NK-cell numbers and pCR to HER2 antibody-based treatment was independent from the CD16A 158 V/F genotype in multivariate analysis [%CD57$^+$ NK OR 1.06 (95% CI 1.0–1.1), $P = 0.004$; CD57$^+$ NK cells/µL OR 1.006 (95% CI 1.0–1.01), $P = 0.01$]. Hence, although not pointing to the specific mechanism, these data rule out the possibility that the CD16 158 V/F genotype influences the association between circulating CD57$^+$ NK cells and pCR neoadjuvant therapy with HER2-specific antibodies.

Comparison of CD57$^+$ cells in tumor-associated and circulating NK-cell populations

Given the inverse association between circulating CD57$^+$ NK cell numbers and pathologic responses to HER2-specific therapeutic antibodies, we sought to investigate whether these cells could be detected in tumor-associated infiltrates from breast carcinomas. Single-cell suspensions were obtained from pretreatment tumor specimens and paired peripheral blood samples followed by the analysis of CD57 and CD16 expression in NK cells by multiparametric flow cytometry. Unbiased analysis of flow cytometry data was performed using t-distributed SNE (t-SNE; ref. 35), which clusters cells by the expression of analyzed parameters in two-dimensional maps. Maps integrating data from circulating and tumor-associated lymphocyte samples ($n = 6$ of each) revealed three clusters of CD57$^+$ lymphocytes corresponding to CD16$^+$ NK cells (1), CD8$^+$ T cells (2), and a minor fraction of CD4$^+$ T cells (3; Fig. 3A). Density maps separately depicting circulating and tumor-associated lymphocytes revealed the predominance of CD57$^+$ NK cells in peripheral blood samples (Fig. 3B). Tumor-associated immune cell infiltrates displayed a consistent reduction in the frequency of NK cells, identified as CD56$^+$CD3$^-$ lymphocytes (Fig. 3C). The percentage of CD16$^+$ tumor-associated NK cells was reduced (Fig. 3D), related to a preferential decrease in CD16$^+$ CD57$^+$ NK-cell fraction (Fig. 3E and F). Lower proportions of CD57$^+$ CD8$^+$ T cells were detected in tumor-associated (18% average frequency) as compared with circulating (42% average frequency) lymphocyte samples.

Chemokine receptors, ADCC, and proliferation of circulating CD57$^+$ NK cells

Limited homing and/or decreased proliferation/survival in the tumor niche could underlie the reduced presence of CD57$^+$ NK cells in breast carcinoma infiltrates. On that basis, we analyzed the expression of CXCR3, CXCR1, and CX3CR1 in circulating CD57$^+$ and CD57$^-$ CD56^{dim} NK cells from patients with HER2$^+$ breast cancer ($n = 6$). CD57$^+$ NK cells showed higher expression of CXCR1 and CX3CR1 compared with CD57$^-$ NK cells, yet expressed lower CXCR3 levels (Fig. 4A–C), a chemokine receptor involved in intratumoral NK-cell accumulation in experimental models (43). Expression of CCR7 and CD62L, markers associated with lymph node homing, was low in CD57$^+$ and CD57$^-$ circulating CD56^{dim} NK cells from patients with HER2$^+$ breast cancer (Fig. 4B and C), in agreement with the chemokine receptor profile previously described in CD56^{dim} NK cells (44). On the other hand, CFSE dilution *in vitro* assays with purified NK cells from healthy donors showed that CD57$^+$ NK cells displayed reduced IL2-dependent proliferation upon activation by CD16 crosslinking with high and low doses of an agonistic mAb, as compared with CD57$^-$ NK cells (Fig. 4D and E) as well as upon activation by soluble IL2, in agreement with published data (24, 30). Lower

Published OnlineFirst June 12, 2019; DOI: 10.1158/2326-6066.CIR-18-0896

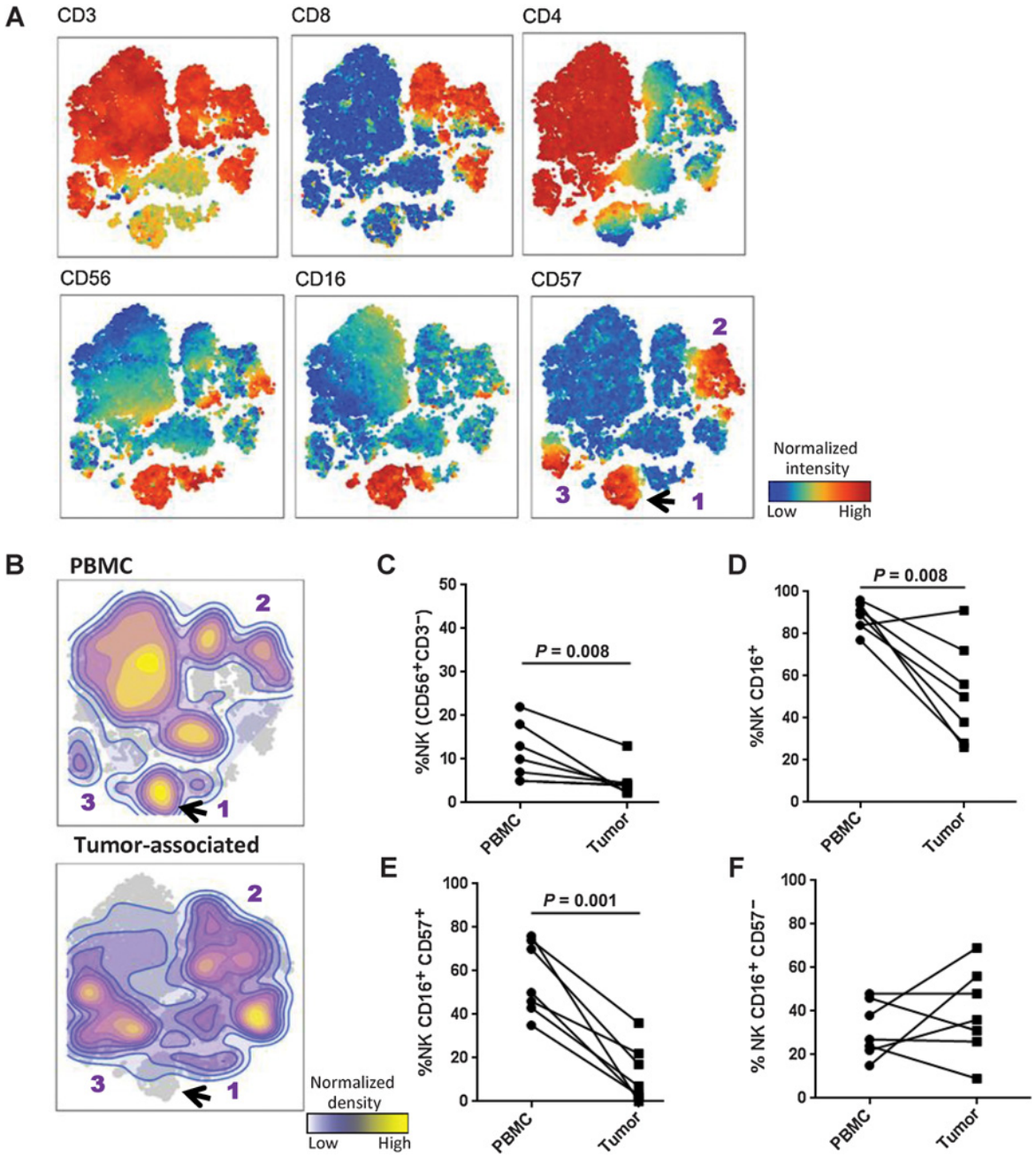

Figure 3.

Reduced presence of CD57$^+$ lymphocytes in tumor-associated as compared with circulating paired samples from patients with breast cancer. Tumor-associated immune cells, isolated by mechanical and enzymatic digestion, and paired PBMC samples, isolated by Ficoll gradient, were analyzed by multiparametric flow cytometry. CD45$^+$ DAPI$^-$ cells with lymphocyte morphology were gated for further analysis. **A,** t-SNE plot showing lymphocyte clusters defined by CD3, CD8, CD4, CD56, CD16, and CD57 expression in circulating and tumor-associated lymphocyte samples. Color scale represents high expression (red) or low expression (blue) of the indicated marker. Numbers indicate the CD57$^+$CD16$^+$ NK-cell cluster (1), the CD57$^+$ CD8$^+$ T-cell cluster (2), and the CD57$^+$CD4$^+$ T-cell cluster (3). **B,** Density maps in the t-SNE field displaying peripheral blood-derived (top) or tumor-associated (bottom) samples compiled separately. **C–F,** Proportions of NK cells (CD56$^+$ CD3$^-$), CD16$^+$ NK cells, CD16$^+$ CD57$^+$, and CD16$^+$CD57$^-$ NK cells in paired circulating and tumor-associated samples from patients with breast cancer ($n = 7$). Statistical significance by Mann–Whitney U test.

CD57$^+$ NK-cell numbers were recovered upon CD16-triggered activation as compared with nontreated or IL2-activated cultures (Fig. 4F).

On the other hand, NK cells from patients with HER2$^+$ breast cancer with high and low proportions of CD57$^+$ NK cells displayed enhanced degranulation and TNFα production

Published OnlineFirst June 12, 2019; DOI: 10.1158/2326-6066.CIR-18-0896

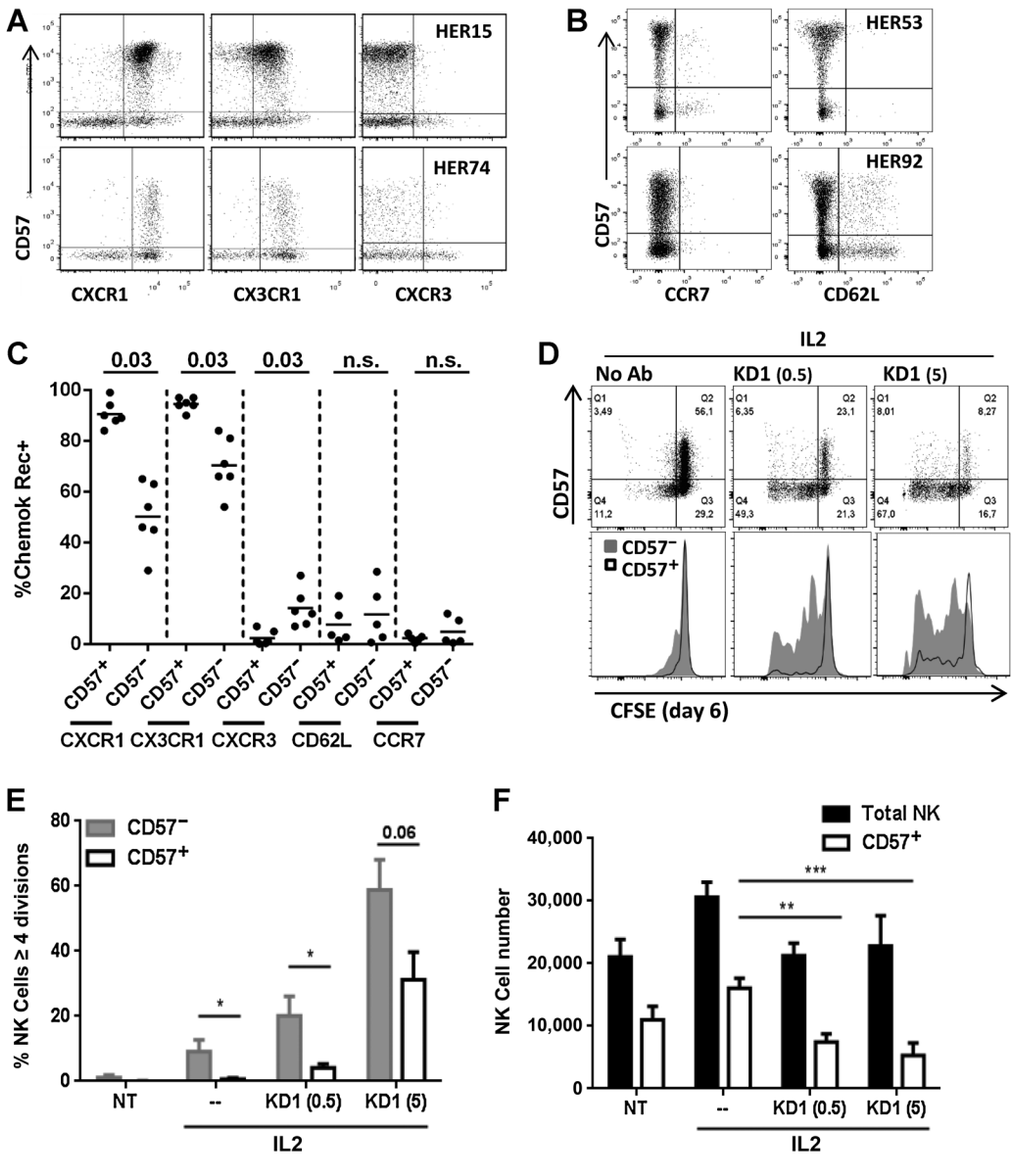

Figure 4.

Circulating CD57$^+$ NK cells show reduced CXCR3 expression and CD16-induced proliferation. Surface expression of CXCR1, CXCR3, CX3CR1, CCR7, and CD62L was analyzed by multiparametric flow cytometry in CD57$^+$ and CD57$^-$ CD56^{dim} NK cells from patients with HER2$^+$ breast cancer. **A** and **B,** Dot plots showing CXCR1, CX3CR1, CXCR3, CCR7, CD62L, and CD57 coexpression in circulating NK cells. Data from four representative patients. **C,** Proportions of CD57$^+$ and CD57$^-$ NK cells positive for each molecule. Each dot represents a single determination in individual patients ($n = 6$). Statistical comparison by Wilcoxon paired test**. D–F,** CFSE dilution assays by flow cytometry using purified NK cells from healthy volunteers cultured for 6 days with plate bound anti-CD16 agonist at 0.5 or 5 μg/mL in the presence of IL2. **D,** Dot plots and histograms showing CFSE labeling in CD57$^+$ and CD57$^-$ NK cells in the indicated conditions. Data from a representative experiment out of 6 performed are shown. **E,** Percentage of CD57$^+$ and CD57$^-$ NK cells $\geq$ 4 divisions at day 6 (mean $\pm$ SEM; $n = 6$). **F,** Numbers of total and CD57$^+$ NK cells recovered at day 6 (mean $\pm$ SEM; $n = 6$).

in *in vitro* ADCC assays against trastuzumab-coated SKBR3 cells (Fig. 5A–C), in accordance with the recognized ADCC proficiency of CD57$^+$ NK cells (30). Indeed, circulating CD57$^+$ NK cells tended to display enhanced trastuzumab-induced degranulation as compared with their CD57$^-$ counterparts in patients with HER2$^+$ breast cancer, showing a comparable profile with that detected in healthy individuals paired by CD16 158 V/F genotype and NKG2C$^+$ adaptive NK-cell content (Fig. 5D-G).

Inverse relation of tumor-infiltrating and circulating CD57$^+$ NK-cell numbers

We have previously described the association between tumor-infiltrating NK-cell (TI-NK) numbers and pCR achievement in patients with early HER2$^+$ breast cancer treated with HER2-specific antibody-based neoadjuvant therapy (12). We analyzed the relationship between circulating CD57$^+$ NK cells and TI-NK-cell numbers in the group of patients for whom those determinations in baseline tumor biopsies were

Published OnlineFirst June 12, 2019; DOI: 10.1158/2326-6066.CIR-18-0896

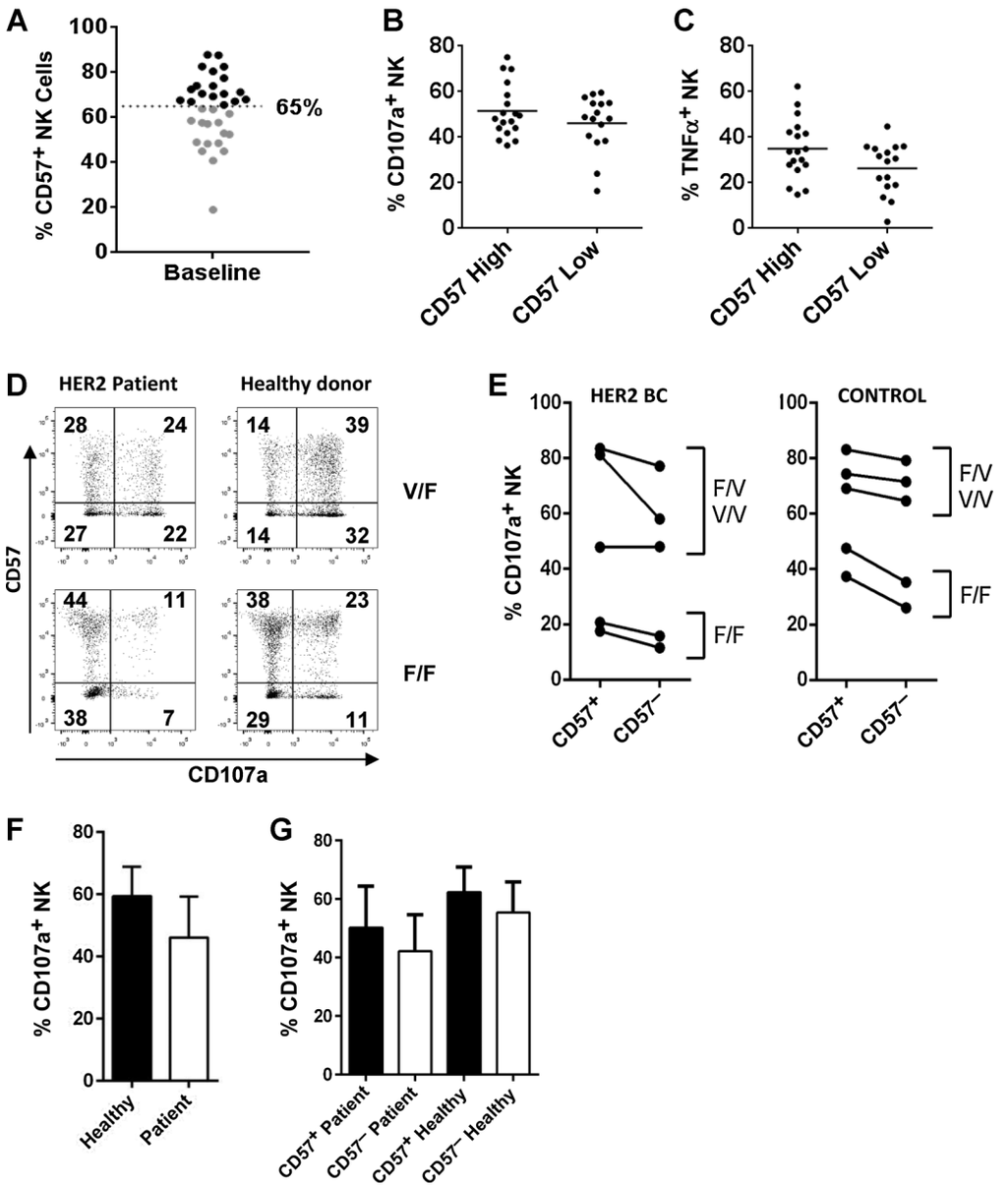

Figure 5.

Comparable responses of CD57$^+$ and CD57$^-$ circulating NK cells from HER2$^+$ breast cancer patients in trastuzumab-induced ADCC *in vitro* assays. **A–C**, NK-cell activation as analyzed in baseline PBMC samples from patients with HER2$^+$ breast cancer by flow cytometry upon coculture with trastuzumab-coated SKBR3 cells. **A,** Frequencies of CD57$^+$ NK cells in PBMC samples from patients categorized as CD57^{high} ($\geq$65% CD57$^+$ NK cells, $n = 18$) or CD57^{low} (<65% of CD57$^+$ NK cells, $n = 16$). **B** and **C,** Percentage of CD107a$^+$ or TNFα^+ CD56^{dim} NK cells in patients with high or low proportions of CD57$^+$ NK cells. *P* values calculated by Mann–Whitney *U* test. **D–G,** PBMCs from patients with HER2$^+$ breast cancer and healthy controls paired by their CD16 genotype and NKG2C profile were cocultured with trastuzumab-coated SKBR3 for 4 hours and degranulation was analyzed by CD107a mobilization assay by flow cytometry (**D**). Dot plots showing the proportions of CD107a$^+$ NK cells according to CD57 expression in NK cells from patients and controls paired by their CD16 genotype. Data from two representative examples are shown. **E–G,** Percentage of total as well as CD57$^+$ and CD57$^-$ NK cells degranulating against trastuzumab-coated SKBR3 cells in PBMC samples from healthy controls and patients with HER2$^+$ breast cancer. Control and patient samples with the same CD16 genotype were assayed in parallel.

already available ($n = 40$; Fig. 6A). In this fraction of the studied cohort, TI-NK-cell numbers in the tumor biopsy and CD57$^+$ circulating NK cells maintained an inverse and independent association with pCR to HER2 therapeutic antibodies (Supplementary Fig. S6). The correlation of both parameters evidenced the existence of a fraction of patients with high CD57$^+$ circulating NK-cell numbers and lacking tumor-infiltrating NK cells (Fig. 6B). TI-NK-cell–associated and CD57–associated cutoffs complemented each other in the identification of patients with primary resistance (high CD57$^+$ NK cells in circulation) or pCR achievement (high TI-NK cells) to HER2-specific therapeutic antibodies. (Fig. 6C and D).

Published OnlineFirst June 12, 2019; DOI: 10.1158/2326-6066.CIR-18-0896

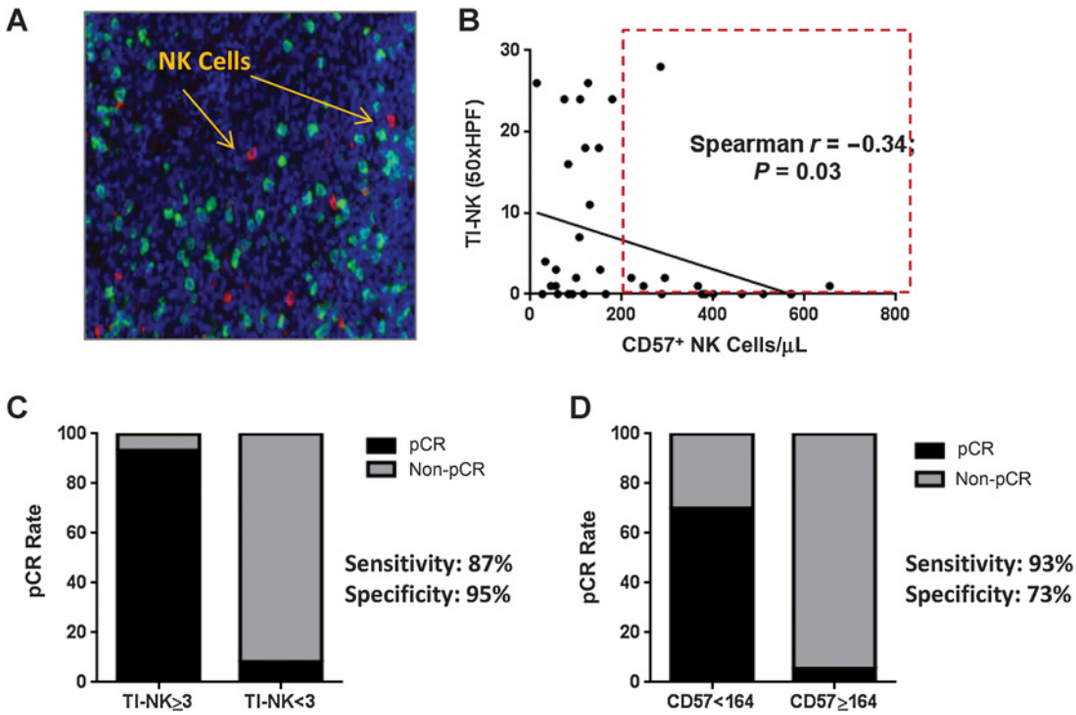

Figure 6.

Circulating CD57$^+$ and tumor-infiltrating NK-cell numbers, respectively, predict resistance and complete response to HER2 therapeutic antibodies. Association between circulating CD57$^+$ NK cells, tumor-infiltrating NK-cell numbers and pCR analyzed in a fraction of patients for whom both parameters were available ($n = 40$). **A,** IHC staining of NK cells identified as CD56$^+$ (red) CD3$^-$ (green) lymphocytes on diagnostic tumor biopsies. **B,** Correlation between tumor-infiltrating NK-cell and circulating CD57$^+$ NK-cell numbers. **C** and **D,** pCR rate in patients stratified according to ≥3 TI-NK cell/50× HPF or by ≥164 circulating CD57$^+$ NK cell/μL cutoffs; sensitivity and specificity of both biomarkers are indicated.

Discussion

The identification of mechanisms influencing the clinical efficacy of tumor antigen–specific antibodies could broaden their therapeutic benefit. We have described tumor-infiltrating NK cells associated with the antitumor efficacy of HER2-specific antibodies in patients with HER2$^+$ breast cancer with primary disease (12). Results herein reported extend our previous findings by describing an inverse association between circulating CD57$^+$ NK-cell numbers and the achievement of pCRs to early treatment with HER2 therapeutic antibodies. Prior studies have evaluated the association between the efficacy of HER2 antibody–based therapies and the magnitude of NK-cell cytotoxicity in *in vitro* assays (10, 45) or genetic factors such as CD16 polymorphisms (41, 42). Our study evidences that the differentiation profile of the circulating NK-cell repertoire correlates with response to HER2 antibody-based therapy, regardless of their cytolytic proficiency *in vitro* or CD16A 158 V/F genotype. From a clinical perspective, baseline screening for high circulating CD57$^+$ NK cells could be implemented for the identification of patients with primary resistance to neoadjuvant treatment with HER2 therapeutic antibodies, complementing the positive predictive value of tumor-infiltrating NK-cell enumeration in diagnostic biopsies. Our results also provide a rationale for testing circulating CD57$^+$ NK cells as biomarker of resistance to tumor antigen–specific antibody-based treatment in other cancer contexts.

The CD57 epitope is a sulfated carbohydrate posttranslationally added to glycoproteins and/or glycolipids on terminally differentiated NK and T cells (30, 46). The fact that patients showed comparable frequencies of total CD57$^+$ T cells and CD57$^+$/CD28$^-$ CD8$^+$ T lymphocytes regardless of pCR status indicated that resistance to HER2-specific antibodies was not associated with general immune senescence or immune risk profiles associated with frailty (47), but rather identified patients with a highly differentiated NK-cell compartment. Prior studies described associations between increased frequencies of circulating CD57$^+$ CD8$^+$ T cells and poor prognosis in several solid tumors (48–50), suggesting that CD57$^+$ CD8$^+$ T cells are unable to control tumor growth despite their cytotoxic activity. Our results indicate that CD57$^+$ NK cells associate to a similarly low capacity for controlling tumor growth in the context of HER2 antibody–based breast cancer treatment. The relationship between circulating CD57$^+$ NK-cell numbers and HER2-specific antibody efficacy is supported by observations showing the reduced presence of tumor-associated CD57$^+$ NK cells and, particularly, the inverse correlation between circulating CD57$^+$ and tumor-infiltrating NK-cell numbers.

Unraveling the molecular keys underlying the herein described association could point to strategies for counteracting primary resistance to HER2 therapeutic antibodies in patients with breast cancer with high numbers of CD57$^+$ circulating NK cells. In the nervous system, CD57 labels proteins involved in cell adhesion,

Published OnlineFirst June 12, 2019; DOI: 10.1158/2326-6066.CIR-18-0896

recognition, and migration, such as NCAM (51). Studies on chemokine receptor expression showed that $CD57^+$ circulating NK cells from patients with $HER2^+$ breast cancer expressed reduced surface CXCR3, a receptor involved in NK-cell tumor homing (43). Reduced CXCR3-dependent homing into breast carcinomas could be one of the mechanisms contributing to $CD57^+$ NK-cell scarcity in tumor immune infiltrates. In addition, circulating $CD57^+$ NK cells displayed limited proliferation and persistence upon activation via CD16 *in vitro*, in agreement with the described replicative senescence of $CD57^+$ T cells (24, 52). Thus, reduced presence of $CD57^+$ NK cells in tumor immune infiltrates and their association with resistance to treatment with HER2 antibodies could also result from their inability to proliferate and persist upon activation in the tumor microenvironment. $CD57^+$ NK cells from patients with $HER2^+$ breast cancer displayed proficient degranulation and cytokine production in response to trastuzumab-coated SKBR3 cells in ADCC *in vitro* assays, indicating that their association with anti-HER2 therapy failure could not be attributed to functional dysfunction but rather depended on features associated with their differentiation stage (i.e., homing and persistence into the tumor). The fact that the efficacy of HER2 therapeutic antibodies was unrelated to the distribution of other receptors related to NK-cell functional maturation (i.e., $NKG2A^+$, KIR^+) or enhanced ADCC *in vitro* (i.e., adaptive $NKG2C^+$ and $Fc\gamma^-$ NK cells) further supported that $CD57^+$ NK-cell association with anti-HER2 efficacy was independent of the cells' functional competence. It is tempting to speculate that differentiated $CD57^+$ NK cells might preferentially home to bone marrow, as suggested by their presence in the bone marrow from patients with leukemia in complete remission (53) and their association with reduced relapse rates in hematopoietic stem cell–transplanted patients (54, 55), while showing reduced surveillance of peripheral tissues. Monitoring changes in tumor-infiltrating NK-cell subpopulations after treatment could provide valuable information on the molecular keys underlying the correlation between $CD57^+$ circulating NK cells and efficacy of HER2-specific antibody-based therapy. However, the nature of this clinical study based on the analysis of samples obtained from patients receiving standard neoadjuvant treatment limits the possibility of studying sequential tumor samples.

Although factors triggering CD57 expression in NK cells are unknown, CD57 expression is enhanced through chronic stimulation by environmental events: $CD57^+$ NK cells increase with age, and show delayed appearance in hematopoietic stem cell transplant recipients (24, 26–28). Chronic viral infections, particularly HCMV, have been associated with $CD57^+$ increased expression in both NK and $CD8^+$ T cells (27, 39, 56, 57). Nonetheless, the association between $CD57^+$ NK cells and response to treatment with HER2 antibodies in the studied patient cohort was independent of chronologic age and uncoupled from changes associated with HCMV infection in both NK- and T-cell compartments (i.e., expansions of $NKG2C^+$ or Fcγ-deficient adaptive NK cells, expression of LILRB1, or inflation of $CD28^-$ or $CD57^+$ effector memory $CD8^+$ T cells). Hence, our data support a model in which the CD57 expression profile in an adult NK-cell compartment is determined by a combination of environmental factors, including not only HCMV infection but also other infections (e.g., EBV) and/or different stimuli (e.g., immunocomplexes). The fact that $CD57^+$ NK-cell numbers were not associated with any clinicopathologic factor (i.e., tumor size, tumor grade, hormone receptor status) argues against the influence of underlying disease on the NK-cell differentiation profile in the studied cohort. Nonetheless, the analysis of other activating (e.g., NKG2D, NKp30, NKp44, or DNAM-1) and inhibitory receptors (e.g., TIGIT and TIM-3) would provide a broader view of NK-cell receptor repertoire in patients with breast cancer.

Circulating $CD57^+$ NK-cell numbers and CD16A genotype could exert a complementary impact on HER2 therapeutic antibody efficacy by influencing NK-cell tumor homing/persistence and the strength of HER2 antibody–dependent activation. Studies on larger cohorts could address whether the combination of variables would provide added value for predicting treatment efficacy.

Limitations of this study include the modest cohort size and the short clinical follow-up that (i) may explain why the trend for CD16A 158 V/F genotype and pCR failed to reach statistical significance and (ii) precluded conclusive association of $CD57^+$ NK cells with long-term treatment efficacy. On the other hand, our study's strengths are the hypothesis-driven prospective design, the progression from previous results relating NK cells to anti-HER2 efficacy in primary breast cancer, and the integration of *in vitro* and *ex vivo* data.

Overall, our data indicate that highly differentiated NK-cell repertoires, revealed by the frequency of $CD57^+$ cells, identify patients with $HER2^+$ breast cancer with resistance to anti-HER2 therapy. The study also identifies NK-cell differentiation status, rather than their functional maturation, as a parameter that might influence on their antitumor function in the context of solid tumors. These results encourage future research extending the analysis of $CD57^+$ NK cells as putative efficacy biomarkers and introducing NK-cell aging as a target for improving the efficacy of HER2-specific therapeutic antibodies.

Disclosure of Potential Conflicts of Interest

A. Muntasell has received speakers bureau honoraria from Roche. B. Bermejo is a consultant/advisory board member for Roche and Pfizer. M. Martinez-Garcia is a consultant/advisory board member for Roche and Pfizer. A. Lluch is a consultant/advisory board member for Novartis, Pfizer, Roche/Genentech, Eisai, and Celgene. J. Albanell reports receiving speakers bureau honoraria and is a consultant/advisory board member for Roche. No potential conflicts of interest were disclosed by the other authors.

Authors' Contributions

Conception and design: A. Muntasell, S. Servitja, F. Rojo, J. Albanell, M. López-Botet

Development of methodology: A. Muntasell, S. Servitja, B. Bermejo, F. Rojo, O. Arpí, L. Soria

Acquisition of data (provided animals, acquired and managed patients, provided facilities, etc.): S. Servitja, M. Cabo, B. Bermejo, S. Perez-Buira, F. Rojo, O. Arpí, M. Moraru, L. Serrano, I. Tusquets, M.T. Martínez, A. Vera, M. Martínez-García, L. Soria, L. Comerma, S. Santana-Hernández, P. Eroles, C. Vilches, A. Lluch

Analysis and interpretation of data (e.g., statistical analysis, biostatistics, computational analysis): A. Muntasell, M. Cabo, F. Rojo, M. Costa-Garcia, G. Heredia, S. Santana-Hernández, J. Albanell, M. López-Botet

Writing, review, and/or revision of the manuscript: A. Muntasell, S. Servitja, M. Cabo, F. Rojo, I. Tusquets, M.T. Martínez, M. Martínez-García, S. Santana-Hernández, P. Eroles, A. Rovira, A. Lluch, J. Albanell, M. López-Botet

Administrative, technical, or material support (i.e., reporting or organizing data, constructing databases): S. Servitja, F. Rojo, G. Heredia, A. Vera, L. Soria, L. Comerma, S. Santana-Hernández, J. Albanell

Study supervision: A. Muntasell, J. Albanell

Other (interpretation and discussion of results): A. Rovira

Acknowledgments

We acknowledge A. Moretta (University of Genoa, Genoa, Italy), L. Lanier (University of California, San Francisco, San Francisco, CA), and S. Ferrini (National Institute for Cancer Research, Genoa, Italy) for kindly providing mAbs used in this study. The authors thank the technical help of Oscar Fornas (Flow cytometry Core Service at PRBB). We acknowledge Xavier Duran [Consulting Service on Methodology for Biomedical research (AMIB) at IMIM] for assistance in statistical analysis. The authors also thank all clinical professionals (Mar Biobank, INCLIVA Biobank (PT17/0015/0049; B.000768 ISCIII//) and nurses at Hospital del Mar/Hospital Clinic de Valencia Oncology Departments) what provided support to this project. We are also especially grateful to all patients and healthy volunteers participating in this study. The authors are supported by coordinated research projects from Asociación Española contra el Cáncer (GCB15152947MELE) and Proyecto Integrado de Excelencia ISCIII (PIE 2015/00008); M. López-Botet and A. Muntasell are supported by Worldwide Cancer Research Foundation (15-1146) and by Plan Estatal I+D Retos (SAF2016-80363-C2-1-R), Spanish Ministry of Economy and Competitiveness (MINECO, FEDER), and by Generalitat de Catalunya (2017 SGR 888). J. Albanell, A. Rovira, and F. Rojo are supported by ISCiii/FEDER (PI15/00146, PI18/00006, PI18/00382 and CIBERONC) and by Generalitat de Catalunya (2017 SGR 507) and Fundació Privada Cellex (Barcelona). A. Lluch and P. Eroles are supported by ISCiii/FEDER (PI15/01617, PI18/01219 and CIBERONC).

The costs of publication of this article were defrayed in part by the payment of page charges. This article must therefore be hereby marked *advertisement* in accordance with 18 U.S.C. Section 1734 solely to indicate this fact.

Received December 13, 2018; revised April 11, 2019; accepted June 10, 2019; published first June 12, 2019.

References

1. Cerwenka A, Lanier LL. Natural killer cell memory in infection, inflammation and cancer. Nat Rev Immunol 2016;16:112–23.
2. Chiossone L, Vienne M, Kerdiles YM, Vivier E. Natural killer cell immunotherapies against cancer: checkpoint inhibitors and more. Semin Immunol 2017;31:55–63.
3. Malmberg KJ, Carlsten M, Bjorklund A, Sohlberg E, Bryceson YT, Ljunggren HG. Natural killer cell-mediated immunosurveillance of human cancer. Semin Immunol 2017;31:20–29.
4. Moretta L, Pietra G, Montaldo E, Vacca P, Pende D, Falco M, et al. Human NK cells: from surface receptors to the therapy of leukemias and solid tumors. Front Immunol 2014;5:87.
5. Muntasell A, Cabo M, Servitja S, Tusquets I, Martinez-Garcia M, Rovira A, et al. Interplay between natural killer cells and anti-HER2 antibodies: perspectives for breast cancer immunotherapy. Front Immunol 2017;8:1544.
6. Bottcher JP, Bonavita E, Chakravarty P, Blees H, Cabeza-Cabrerizo M, Sammicheli S, et al. NK cells stimulate recruitment of cDC1 into the tumor microenvironment promoting cancer immune control. Cell 2018;172:1022–37.
7. Clynes RA, Towers TL, Presta LG, Ravetch JV. Inhibitory Fc receptors modulate in vivo cytotoxicity against tumor targets. Nat Med 2000;6:443–6.
8. Park S, Jiang Z, Mortenson ED, Deng L, Radkevich-Brown O, Yang X, et al. The therapeutic effect of anti-HER2/neu antibody depends on both innate and adaptive immunity. Cancer Cell 2010;18:160–70.
9. Stagg J, Loi S, Divisekera U, Ngiow SF, Duret H, Yagita H, et al. Anti-ErbB-2 mAb therapy requires type I and II interferons and synergizes with anti-PD-1 or anti-CD137 mAb therapy. Proc Natl Acad Sci U S A 2011;108:7142–7.
10. Arnould L, Gelly M, Penault-Llorca F, Benoit L, Bonnetain F, Migeon C, et al. Trastuzumab-based treatment of HER2+ breast cancer: an antibody-dependent cellular cytotoxicity mechanism? Br J Cancer 2006;94:259–67.
11. Muller P, Kreuzaler M, Khan T, Thommen DS, Martin K, Glatz K, et al. Trastuzumab emtansine (T-DM1) renders HER2+ breast cancer highly susceptible to CTLA-4/PD-1 blockade. Sci Transl Med 2015;7:315ra188.
12. Muntasell A, Rojo F, Servitja S, Rubio-Perez C, Cabo M, Tamborero D, et al. NK cell infiltrates and HLA class I expression in primary HER2(+) breast cancer predict and uncouple pathological response and disease-free survival. Clin Cancer Res 2019;25:1535–45.
13. Cooper MA, Fehniger TA, Caligiuri MA. The biology of human natural killer-cell subsets. Trends Immunol 2001;22:633–40.
14. Boudreau JE, Hsu KC. Natural killer cell education and the response to infection and cancer therapy: stay tuned. Trends Immunol 2018;39:222–39.
15. Guma M, Angulo A, Vilches C, Gomez-Lozano N, Malats N, Lopez-Botet M. Imprint of human cytomegalovirus infection on the NK cell receptor repertoire. Blood 2004;104:3664–71.
16. Horowitz A, Djaoud Z, Nemat-Gorgani N, Blokhuis J, Hilton HG, Beziat V, et al. Class I HLA haplotypes form two schools that educate NK cells in different ways. Sci Immunol 2016;1:eaag1672.
17. Muntasell A, Vilches C, Angulo A, Lopez-Botet M. Adaptive reconfiguration of the human NK-cell compartment in response to cytomegalovirus: a different perspective of the host-pathogen interaction. Eur J Immunol 2013;43:1133–41.
18. Costa-Garcia M, Vera A, Moraru M, Vilches C, Lopez-Botet M, Muntasell A. Antibody-mediated response of NKG2Cbright NK cells against human cytomegalovirus. J Immunol 2015;194:2715–24.
19. Lopez-Montanes M, Alari-Pahissa E, Sintes J, Martinez-Rodriguez JE, Muntasell A, Lopez-Botet M. Antibody-dependent NK cell activation differentially targets EBV-infected cells in lytic cycle and bystander B lymphocytes bound to viral antigen-containing particles. J Immunol 2017;199:656–65.
20. Moraru M, Black LE, Muntasell A, Portero F, Lopez-Botet M, Reyburn HT, et al. NK cell and Ig interplay in defense against herpes simplex virus type 1: epistatic interaction of CD16A and IgG1 allotypes of variable affinities modulates antibody-dependent cellular cytotoxicity and susceptibility to clinical reactivation. J Immunol 2015;195:1676–84.
21. Manser AR, Uhrberg M. Age-related changes in natural killer cell repertoires: impact on NK cell function and immune surveillance. Cancer Immunol Immunother 2016;65:417–26.
22. Tarazona R, Sanchez-Correa B, Casas-Aviles I, Campos C, Pera A, Morgado S, et al. Immunosenescence: limitations of natural killer cell-based cancer immunotherapy. Cancer Immunol Immunother 2017;66:233–45.
23. Ong E, Yeh JC, Ding Y, Hindsgaul O, Pedersen LC, Negishi M, et al. Structure and function of HNK-1 sulfotransferase. Identification of donor and acceptor binding sites by site-directed mutagenesis. J Biol Chem 1999;274:25608–12.
24. Bjorkstrom NK, Riese P, Heuts F, Andersson S, Fauriat C, Ivarsson MA, et al. Expression patterns of NKG2A, KIR, and CD57 define a process of CD56dim NK-cell differentiation uncoupled from NK-cell education. Blood 2010;116:3853–64.
25. Lanier LL, Le AM, Phillips JH, Warner NL, Babcock GF. Subpopulations of human natural killer cells defined by expression of the Leu-7 (HNK-1) and Leu-11 (NK-15) antigens. J Immunol 1983;131:1789–96.
26. Abo T, Miller CA, Balch CM. Characterization of human granular lymphocyte subpopulations expressing HNK-1 (Leu-7) and Leu-11 antigens in the blood and lymphoid tissues from fetuses, neonates and adults. Eur J Immunol 1984;14:616–23.
27. Krishnaraj R, Svanborg A.Preferential accumulation of mature NK cells during human immunosenescence. J Cell Biochem 1992;50:386–91.
28. Le Garff-Tavernier M, Beziat V, Decocq J, Siguret V, Gandjbakhch F, Pautas E, et al. Human NK cells display major phenotypic and functional changes over the life span. Aging Cell 2010;9:527–35.
29. Nielsen CM, White MJ, Goodier MR, Riley EM. Functional significance of CD57 expression on human NK cells and relevance to disease. Front Immunol 2013;4:422.
30. Lopez-Verges S, Milush JM, Pandey S, York VA, Arakawa-Hoyt J, Pircher H, et al. CD57 defines a functionally distinct population of mature NK cells in the human CD56dimCD16+ NK-cell subset. Blood 2010;116:3865–74.

Published OnlineFirst June 12, 2019; DOI: 10.1158/2326-6066.CIR-18-0896

31. Koene HR, Kleijer M, Algra J, Roos D, von dem Borne AE, de HM. Fc gammaRIIIa-158V/F polymorphism influences the binding of IgG by natural killer cell Fc gammaRIIIa, independently of the Fc gammaRIIIa-48L/R/H phenotype. Blood 1997;90:1109–14.
32. Wolff AC, Hammond ME, Hicks DG, Dowsett M, McShane LM, Allison KH, et al. Recommendations for human epidermal growth factor receptor 2 testing in breast cancer: American Society of Clinical Oncology/College of American Pathologists clinical practice guideline update. J Clin Oncol 2013;31:3997–4013.
33. Ogston KN, Miller ID, Payne S, Hutcheon AW, Sarkar TK, Smith I, et al. A new histological grading system to assess response of breast cancers to primary chemotherapy: prognostic significance and survival. Breast 2003;12:320–7.
34. Vilches C, Castano J, Munoz P, Penalver J. Simple genotyping of functional polymorphisms of the human immunoglobulin G receptors CD16A and CD32A: a reference cell panel. Tissue Antigens 2008;71:242–6.
35. Amir el-AD, Davis KL, Tadmor MD, Simonds EF, Levine JH, Bendall SC, et al. viSNE enables visualization of high dimensional single-cell data and reveals phenotypic heterogeneity of leukemia. Nat Biotechnol 2013;31:545–52.
36. Broglio KR, Quintana M, Foster M, Olinger M, McGlothlin A, Berry SM, et al. Association of pathologic complete response to neoadjuvant therapy in HER2+ breast cancer with long-term outcomes: a meta-analysis. JAMA Oncol 2016;2:751–60.
37. Bengner M, Beziat V, Ernerudh J, Nilsson BO, Lofgren S, Wikby A, et al. Independent skewing of the T cell and NK cell compartments associated with cytomegalovirus infection suggests division of labor between innate and adaptive immunity. Age 2014;36:571–82.
38. Goodier MR, White MJ, Darboe A, Nielsen CM, Goncalves A, Bottomley C, et al. Rapid NK cell differentiation in a population with near-universal human cytomegalovirus infection is attenuated by NKG2C deletions. Blood 2014;124:2213–22.
39. Hassouneh F, Lopez-Sejas N, Campos C, Sanchez-Correa B, Tarazona R, Solana R, et al. Differential effect of cytomegalovirus infection with age on the expression of CD57, CD300a, and CD161 on T-cell subpopulations. Front Immunol 2017;8:649.
40. Gavin PG, Song N, Kim SR, Lipchik C, Johnson NL, Bandos H, et al. Association of polymorphisms in FCGR2A and FCGR3A with degree of trastuzumab benefit in the adjuvant treatment of ERBB2/HER2+ breast cancer: analysis of the NSABP B-31 trial. JAMA Oncol 2017;3:335–41.
41. Hurvitz SA, Betting DJ, Stern HM, Quinaux E, Stinson J, Seshagiri S, et al. Analysis of Fcgamma receptor IIIa and IIa polymorphisms: lack of correlation with outcome in trastuzumab-treated breast cancer patients. Clin Cancer Res 2012;18:3478–86.
42. Musolino A, Naldi N, Bortesi B, Pezzuolo D, Capelletti M, Missale G, et al. Immunoglobulin G fragment C receptor polymorphisms and clinical efficacy of trastuzumab-based therapy in patients with HER-2/neu+ metastatic breast cancer. J Clin Oncol 2008;26:1789–96.
43. Wendel M, Galani IE, Suri-Payer E, Cerwenka A. Natural killer cell accumulation in tumors is dependent on IFN-gamma and CXCR3 ligands. Cancer Res 2008;68:8437–45.
44. Berahovich RD, Lai NL, Wei Z, Lanier LL, Schall TJ. Evidence for NK cell subsets based on chemokine receptor expression. J Immunol 2006;177:7833–40.
45. Varchetta S, Gibelli N, Oliviero B, Nardini E, Gennari R, Gatti G, et al. Elements related to heterogeneity of antibody-dependent cell cytotoxicity in patients under trastuzumab therapy for primary operable breast cancer overexpressing Her2. Cancer Res 2007;67:11991–9.
46. Kared H, Martelli S, Ng TP, Pender SL, Larbi A. CD57 in human natural killer cells and T-lymphocytes. Cancer Immunol Immunother 2016;65:441–52.
47. Larbi A, Franceschi C, Mazzatti D, Solana R, Wikby A, Pawelec G. Aging of the immune system as a prognostic factor for human longevity. Physiology 2008;23:64–74.
48. Akagi J, Baba H.Prognostic value of CD57(+) T lymphocytes in the peripheral blood of patients with advanced gastric cancer. Int J Clin Oncol 2008;13:528–35.
49. Characiejus D, Pasukoniene V, Jonusauskaite R, Azlauskaite N, Aleknavicius E, Mauricas M, et al. Peripheral blood CD8highCD57+ lymphocyte levels may predict outcome in melanoma patients treated with adjuvant interferon-alpha. Anticancer Res 2008;28:1139–42.
50. Characiejus D, Pasukoniene V, Jacobs JJ, Eidukevicius R, Jankevicius F, Dobrovolskiene N, et al. Prognostic significance of peripheral blood CD8highCD57+ lymphocytes in bladder carcinoma patients after intravesical IL-2. Anticancer Res 2011;31:699–703.
51. Kunemund V, Jungalwala FB, Fischer G, Chou DK, Keilhauer G, Schachner M. The L2/HNK-1 carbohydrate of neural cell adhesion molecules is involved in cell interactions. J Cell Biol 1988;106:213–23.
52. Brenchley JM, Karandikar NJ, Betts MR, Ambrozak DR, Hill BJ, Crotty LE, et al. Expression of CD57 defines replicative senescence and antigen-induced apoptotic death of CD8+ T cells. Blood 2003;101:2711–20.
53. Sorskaar D, Forre O, Lie SO. Increased natural killer cell activity and numbers of Leu-7 and Leu-11b (CD 16)+ cells in bone marrow of children in remission from acute lymphoblastic leukaemia. Scand J Immunol 1989;29:65–72.
54. Cichocki F, Cooley S, Davis Z, DeFor TE, Schlums H, Zhang B, et al. CD56dimCD57+NKG2C+ NK cell expansion is associated with reduced leukemia relapse after reduced intensity HCT. Leukemia 2016;30:456–63.
55. Muccio L, Bertaina A, Falco M, Pende D, Meazza R, Lopez-Botet M, et al. Analysis of memory-like natural killer cells in human cytomegalovirus-infected children undergoing alphabeta+T and B cell-depleted hematopoietic stem cell transplantation for hematological malignancies. Haematologica 2016;101:371–81.
56. Bayard C, Lepetitcorps H, Roux A, Larsen M, Fastenackels S, Salle V, et al. Coordinated expansion of both memory T cells and NK cells in response to CMV infection in humans. Eur J Immunol 2016;46:1168–79.
57. Wang EC, Moss PA, Frodsham P, Lehner PJ, Bell JI, Borysiewicz LK. CD8highCD57+ T lymphocytes in normal, healthy individuals are oligoclonal and respond to human cytomegalovirus. J Immunol 1995;155:5046–56.

Published OnlineFirst June 12, 2019; DOI: 10.1158/2326-6066.CIR-18-0896

Cancer Immunology Research

High Numbers of Circulating CD57$^+$ NK Cells Associate with Resistance to HER2-Specific Therapeutic Antibodies in HER2 $^+$ Primary Breast Cancer

Aura Muntasell, Sònia Servitja, Mariona Cabo, et al.

Cancer Immunol Res 2019;7:1280-1292. Published OnlineFirst June 12, 2019.